Proposal, Design, and Performance Investigation of ZnO-Based ISFET pH Sensor

Ankita Porwal, Chitrakant Sahu, and Nawaz Shafi

1 Introduction

In both chemical and biological processes, the measurement of pH is crucial [1, 2]. Although a glass electrode can measure the pH, it has some drawbacks, such as the fragility of glass and less flexibility, so it cannot be employed in the food industry. To measure pH, different types of field effect transistors are modified, such as ion sensitive field effect transistor (ISFET) and extended gate field effect transistor (EGFET), which is reported in the literature [3].

High sensitivity, selectivity, reliability, and affordability are the performance criteria for evaluating pH sensors. Recently, ZnO-based detectors have caught much attention because of the nontoxicity, thermal stability, electrochemical signaling, fast electron transfer, and biocompatibility nature of ZnO [4]. ZnO is a wide-band gap semiconductor and has a high ionic bonding. Zinc oxide as a sensing material is analyzed in many fields, such as chemical sensors, solar cells, electrochemical cells, biosensors, and light-emitting diodes [5, 6]. Apart from sensing hydrogen ion (H^{+}), recently, ZnO-based nanorod FET has been fabricated for the detection of phosphate (PO_4^{-3}), nitrate (NO_3^{-}), and potassium ions (K^{+}) by K. S. Bhat et al. with high sensitivity and selectivity and low detection limits [7]. ZnO as a sensing layer is integrated with EGFET, and this device shows high voltage & current sensitivity (53.21 mV/pH and $-$ 10.43 $\mu A^{1/2}$), respectively [8]. To examine in a noninvasive manner, ZnO-based EGFET was fabricated by sol-gel process, and the device shows a voltage sensitivity of 63.15 mV/pH and linearity of 0.99 [9].

A. Porwal (✉) · C. Sahu
Department of Electronics and Communication Engineering, Malaviya National Institute of Technology Jaipur, Jaipur, Rajasthan 302017, India
e-mail: ankita.sporwal@gmail.com

N. Shafi
School of Electronics Engineering, Vellore Institute of Technology, Vellore, India

T. R. Lenka et al. (eds.), *Micro and Nanoelectronics Devices, Circuits and Systems*,
Lecture Notes in Electrical Engineering 1067,
https://doi.org/10.1007/978-981-99-4495-8_34

The fabrication of the semiconductor-based sensor is the succession of well-established Si Technology [10]. The silicon-based sensor is favorable because of its low cost, reproducibility, and controllable electronic response. However, this sensor cannot work at critical points such as high temperature and pressure. Wide-bandgap semiconductors such as ZnO can replace mature silicon technology because of their attractive properties (biocompatibility, piezoelectric, non- toxicity, stability, and label-free sensing) [11]. ZnO can absorb the protein or enzymes with a low isoelectric point (IEP) of 4.5 because of its high isoelectric point (9.5) [12].

To measure the pH among a variety of biosensors, ISFET is mainly used, which has multiple advantages such as rapid response, small size, low output impedance, highly reliable, and on-chip integration of biosensor arrays [13]. ISFET is employed to detect the enzyme, immune, DNA, and cell-based material used in the healthcare industry, environment monitoring, DNA detection, food industry, and biomedicine that can be easily integrated with microfluidic for sensing applications. In 1970, Bergveld first fabricated the ISFET; since then, continuous modifications have been going on to improve the performance and figure of merits (sensitivity & signal-to-noise ratio) [14].

To overcome the short channel effects, achieve high sensitivity, and attain high switching capability, a conventional sensing layer of ISFET is replaced by a new material ZnO. This structure is a field effect transistor compatible with the CMOS fabrication process. Portability, compactness, simplicity, cheap cost, and ease of manipulating the sensor based on FET enable in situ monitoring [7]. A FET can work as a biosensor by replacing a metal gate electrode with a sensitive layer, which reacts with the solution to be measured. The gate and reference voltage are supplied to provide biasing in the circuit.

In literature, ISFET is characterized through simulation, modeling, and fabrication [15, 16]. ISFET is an electrochemical sensor with chemical input in the form of ion concentration. In an ISFET at interfaces (electrolyte and electrolyte-oxide), an electrochemical reaction happens that helps detect ions. Gouy-Chapman explained this electrochemical reaction in terms of Stern double-layer capacitance [17].

In this paper, in conventional ISFET, gate oxide material SiO_2 is accompanied by ZnO as a sensing layer in addition to junctionless geometry in the structure, significantly improving sensitivity. The design of ISFET is almost similar to MOSFET, where a reference gate replaces the top gate in the electrolyte solution with a sensing membrane. A stern layer surrounds the top gate layer with a capacitance of 20 μF/cm^{-2} and a thin membrane layer.

2 Model Simulation

The projected device's schematic construction is depicted in Fig. 1, and the measurement of various layers in device design is represented in Table 1. The electrolyte solution is considered an intrinsic semiconductor because of similar properties of cations and anions with electrons and holes in the semiconductor. The electrolyte solution

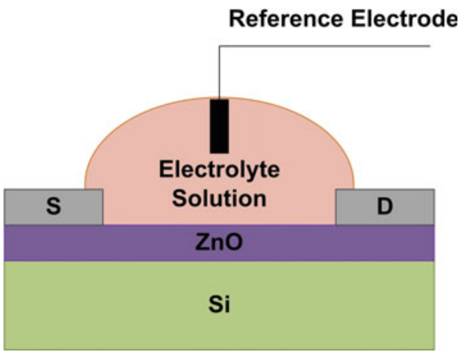

Fig. 1 Schematic structure of proposed ZnO ISFET

Table 1 Measurement of various layers of ZnO ISFET

Parameter name	Symbol	Value
Electrolyte thickness	T_{el}	10 nm
Length of channel	L_{ch}	100 nm
Thickness of oxide	T_{ox}	2 nm
Thickness of silicon	T_{si}	8 nm
Doping in the channel	N_{ch}	1.2×10^{24} m^{-3}
Doping in the source and drain	N_{ch}	1.2×10^{24} m^{-3}
Stern layer thickness	T_{st}	1 nm

is simulated considering the dielectric constant of water ($k = 78$), electron & hole mobility of ZnO, and properties of the ZnO semiconductor (affinity, permittivity, energy bandgap, and density of states) [18]. The intrinsic semiconductor material consists of thermal-generated mobile carriers. The ion molar concentration of the electrolyte solution is defined by the density of states in the conduction and valence bands [19]. The electrolyte solution interacts with the oxide (sensing membrane) and generates surface charges.

The structure consists of a ZnO semiconductor material as a sensing layer, enhancing the figure of merits. The simulation parameters and framework of the proposed device have been maintained coherently with our previous works [20]. A thin membrane layer is also considered between the electrolyte solution and the stern layer. The membrane layer is simulated as silicon with a high dielectric constant ($k = 77.8$), and the density of states in the conduction and valence band is ($N_c = 4.16199 \times 10^{25}$ and $N_v = 3.74 \times 10^{23}$), respectively. The stern layer is considered an oxide of thickness 1 nm and $k = 21$. Various models such as concentration-dependent mobility (conmob), field-dependent mobility (fldmob), Fermi-Dirac model (fermidirac), Shockley-Read-Hall recombination model (srh), and basic model are applied during the simulation of the proposed ISFET. The charge concentration is considered at the interfaces (electrode and electrode/oxide interface) to model the device accurately.

In an ISFET, the concentration of ions can be measured by electrical potential when the sensing layer interacts with an electrolyte solution. The sensitivity parameters can be derived from the site binding model [21]. In the proposed device, ZnO is the insulating layer; when this layer interacts with the pH solution following reaction occurs at the interface:

$$\mathrm{ZnOH} \leftrightarrow \mathrm{ZnO}^- + \mathrm{H}^+ \tag{1}$$

The membrane layer incorporates the charged ions, which are situated between the electrolyte solution and the stern layer. The membrane layer assists in the alignment of the biomolecules to be detected in the sensing layer. Water in an ionized form is represented as

$$\mathrm{H_2O} \leftrightarrow \mathrm{H}^+ + \mathrm{OH}^- \tag{2}$$

The concentration of carrier is described as per Boltzmann Statistics considering holes equal to H ions and electrons equal to hydroxyl ion ($p = [\mathrm{H}^+]$, $n = [\mathrm{OH}^-]$, and $E_c - E_f = E_g/2$). The density of states in the conduction and valence band (N_c and N_v) is defined as

$$N_c = \mathrm{ne}^{\frac{Eg}{2kT}} \tag{3}$$

$$N_v = \mathrm{pe}^{\frac{Eg}{2kT}} \tag{4}$$

The link between density of states in the conduction and valence band and the pH change in the electrolyte solution is established by above equations.

3 Simulation Results and Discussion

The device is characterized at $V_{GS} = 0$–2 V, $V_{DS} = 0.1$ V, and the electrolyte solution contains pH = 3–11. Figure 2 shows the contour plot of potential along the device at all voltages equal to zero ($V_{GS} = V_{DS} = 0$ V). A horizontally cut line is drawn at the surface of ZnO to extract the potential.

The potential fluctuation in the channel region is illustrated in Fig. 3. The sensing performance of the ISFET depends upon the sensing membrane's potential variation. The potential changes with pH according to the site binding model. The variation in potential further leads to variations in the drain-to-source current of ISFET. Site binding theory states that variations in the surface potential voltage at the interface of the aqueous electrolyte solution-sensing layer can result from the concentration of active binding sites on the oxide layer. The surface potential of the sensing layer and pH of the electrolyte solution are related through site binding model, and mathematically, it is represented as [22]:

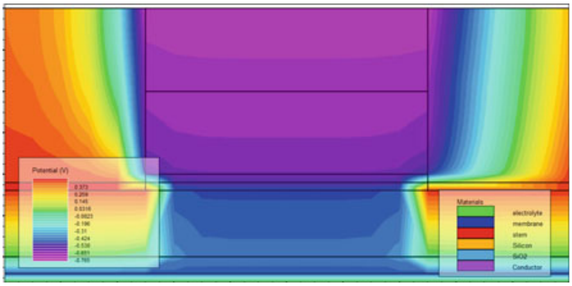

Fig. 2 Contour plot of the variation of potential along the device

$$2.303\left(\mathrm{pH_{pzc}} - \mathrm{pH}\right) = \frac{q\varphi_o}{kT} + \sin h^{-}\frac{q\varphi_o}{kT} * \frac{1}{\beta} \quad (5)$$

where $\mathrm{pH_{PZC}}$ is the pH value at the point of zero charge on the sensing layer, q is for the charge of a single electron, k stands for Boltzmann's constant, T defines the temperature, and β is the sensitivity parameter that indicates the sensitivity of the oxide layer.

The variation of energy in the conduction band and valence band at different pH values ranging from 3 to 11 is shown in Fig. 4. An Ag/AgCl reference electrode is considered, which has stability against variations in the electrolyte solution. The reference electrode is dipped in the pH solution to measure the current at different pH values. The reference electrode supplied a bias to the sensing layer, and the drain current was measured. The drain-to-source voltage value is kept at a low value (0.1 V) to minimize the leakage current. At zero gate voltage, leakage current is almost negligible (10^{-13} A/μm), and at high gate voltage $V_{GS} = 2$ V, the current is in the range of (10^{-5} A/μm). The con- centration of ions varies with pH, so the current is because ions are exchanged between an aqueous electrolyte solution and the sensing surface layer. The device also exhibited a high I_{ON}/I_{OFF} current ratio,

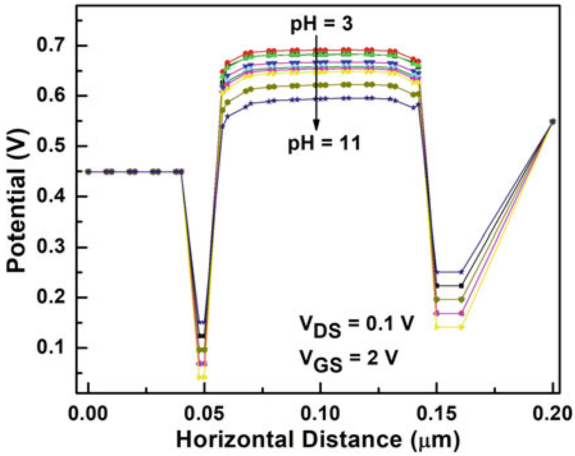

Fig. 3 Variation of potential along with pH solution

i.e., 10^{-8}, as shown in Fig. 5. By dividing the highest on-state current by the most negligible off-state current, the I_{ON}/I_{OFF} ratio is calculated.

At low pH values, the concentration of hydrogen H^+ ions is higher in the solution, accumulating in the oxide interface. More positive voltage is provided to the gate electrode when more positive hydrogen ions are present, boosting the drain current.

The transconductance curve of a ZnO ISFET is shown in Fig. 6 at gate voltage $V_{GS} = 0$–2 V in 0.01 steps, with the variation in pH values ranging from 3 to 11. The transconductance (g_m) is calculated by differentiating Fig. 5 at the constant drain-to-source voltage $V_{DS} = 0.1$ V. g_m values increase at a particular gate voltage, and then, it starts decreasing. The transconductance is highest (0.342 mS/μm) at $V_{GS} = 1.9\ V$ and pH = 11. A high value of g_m denotes the greater drain current change for a given surface charge change.

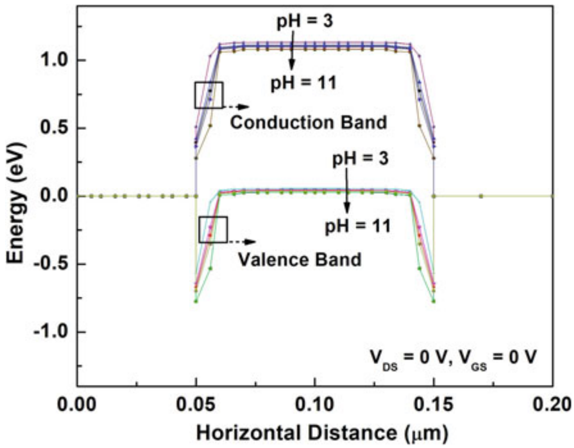

Fig. 4 Energy band diagram of the proposed device in the conduction and valence band

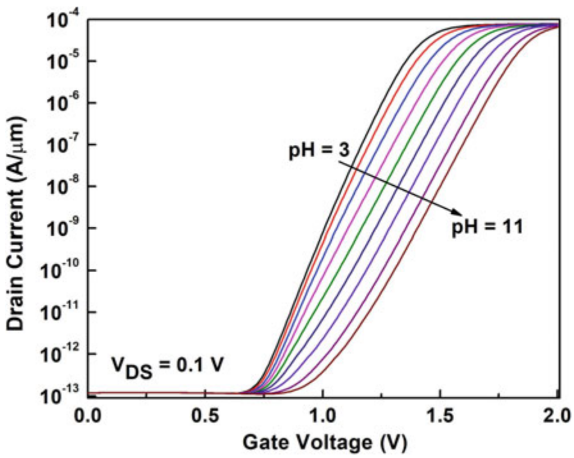

Fig. 5 Transfer characteristics of a ZnO-based ISFET

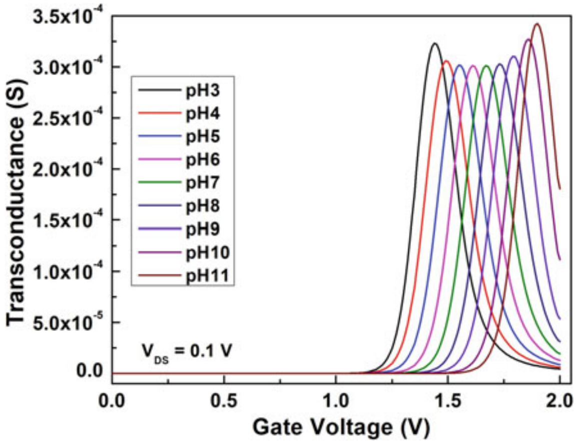

Fig. 6 Transconductance characteristics along with the variation in pH values

4 The Figure of Merits (FOMs)

The proposed device is characterized by various figure of merits (sensitivity, signal-to-noise ratio, and transconductance-to-current ratio).

4.1 Sensitivity

The Nernst equation defines the sensitivity of an ideal biosensor, i.e., 59 mv/pH at room temperature. The Nernst equation is an equation, as shown below, that describes the link between electric potential of the cell membrane and the ionic concentrations that occurred during the electrochemical reaction.

$$E = E_O + 2.303\frac{RT}{nF}\,\text{pH} \tag{6}$$

where E and E_o are the measured and standard potential, respectively, R defines the universal gas constant, T denotes the absolute temperature, n stands for the number of moles of electrons transferred in the electrochemical reaction, and F is the Faraday constant.

The sensitivity of an ideal biosensor is calculated through the Nernst equation which is given as [23]:

$$S_{\text{Ideal}} = 2.303\frac{kT}{q} \approx 59\text{mv/pH} \tag{7}$$

where kT/q defines by the thermal voltage.

In FETs, sensitivity is calculated from FET's characteristics, such as transconductance and the on-off ratio of drain current. The average sensitivity is estimated by the change in threshold voltage and drain current with respect to pH. Threshold voltage varies with pH solutions, as does the concentration of carriers in the solution, which further influences the change in drain current. The threshold voltage sensitivity is defined as

$$SV_{\mathrm{th}} = \frac{V_{\mathrm{th}}(\mathrm{pH2}) - V_{\mathrm{th}}(\mathrm{pH1})}{\mathrm{pH2} - \mathrm{pH1}} = \frac{\Delta V_{\mathrm{th}}}{\Delta \mathrm{pH}} \tag{8}$$

The device's sensitivity is tested with the ZnO layer at various pH solutions (pH = 3–11). The gate voltage ranges from 0 V to 2 V, while the drain voltage is maintained at 0.1 V during the simulation. The electrolyte and oxide interface's properties affect a sensor's sensing ability.

For the calculation of the threshold voltage, a constant current method (10^{-7} * W/L) is used at $V_{DS} = 0.1$ V. Figure 7 represents the voltage sensitivity in the acid medium (pH = 3, 4, 5, and 6) and alkaline medium (pH = 8, 9, 10, and 11). From the voltage sensitivity graph, it can be understood that the device shows 60 mV/pH threshold voltage sensitivity, near the Nernst limit (59 mV/pH).

$$\text{Current Sensitivity } (\Delta I_{\mathrm{DS}}) = \frac{I_{\mathrm{var}} - I_{\mathrm{cons}}(\mathrm{pH} = 7)}{I_{\mathrm{cons}}(\mathrm{pH} = 7)} = \frac{\Delta I_D}{I_D} \tag{9}$$

The current sensitivity of the device in mathematical form is represented in above equation and plotted in acid and alkaline mediums shown in Fig. 8.

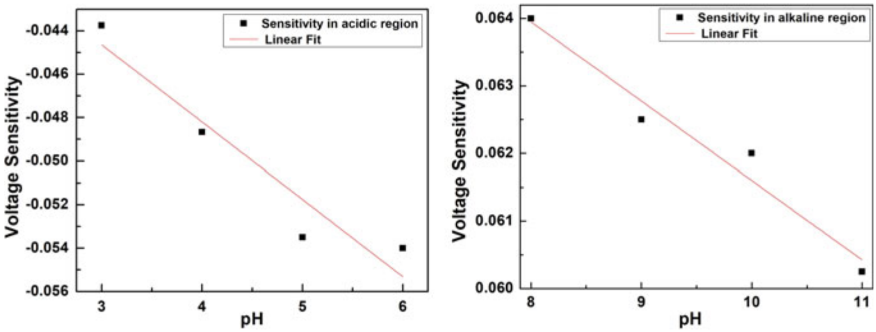

(a) in the acidic solution (b) in the alkaline solution

Fig. 7 Threshold voltage sensitivity

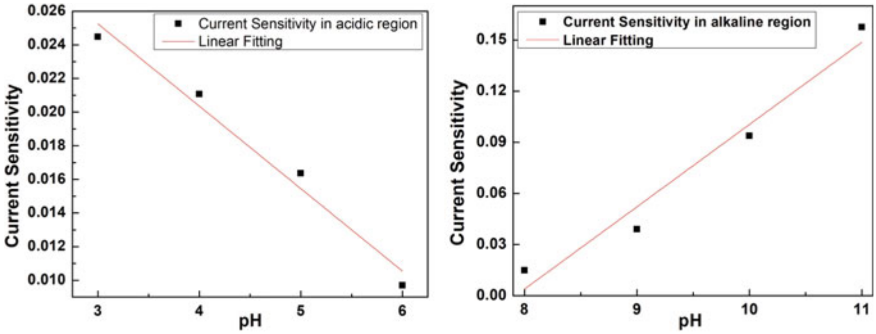

(a) in the acidic solution (b) in the alkaline solution

Fig. 8 Current sensitivity

4.2 Signal-to-Noise Ratio (SNR)

SNR measures the detection ability of a device, and it is defined as the ratio of usable signal to noisy signal. SNR can also be represented by power spectral density (PSD), and in mathematical form, it is described as [24]:

$$\mathrm{SNR} = \frac{\delta I_{\mathrm{us}}}{\delta I_{\mathrm{ns}}} = \frac{\delta I_{\mathrm{us}}}{\sqrt{\int S_I dF}} \tag{10}$$

$$S_{I(f)} = \frac{S^2 \alpha}{f N} \tag{11}$$

where S_I is the power spectral density of the drain current, f is the frequency, N is the carrier concentration, and α is the Hooge constant.

Figure 9 represents the SNR curve of the proposed device at $V_{\mathrm{DS}} = 0.1$ V and $V_{\mathrm{GS}} = 2$ V, and it shows a sharp peak at $V_{\mathrm{GS}} = 1.25$ V. SNR follows the transconductance, and higher SNR shows a lower detection limit of the sensor [25].

4.3 Transconductance-To-Current Ratio (g_m/I_{DS})

g_m/I_{DS} is also applied as a sensing parameter for FET devices to observe the change in ion concentration [26]. g_m/I_{DS} is an analog performance indicator. The transconductance-to-current ratio characteristics of the ZnO ISFET obtained by sweeping gate voltage is shown in Fig. 10. These characteristics follow the pattern of transconductance. It means g_m increases at a fixed voltage, attains a peak value, and then starts decreasing with the increasing gate voltage.

The proposed device is demonstrated through simulation with excellency for pH application and, in future, can be fabricated through a simpler fabrication process. The

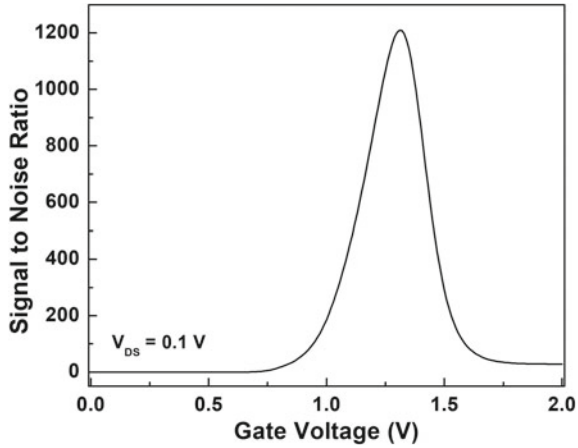

Fig. 9 Signal-to-noise ratio of ZnO-based ISFET

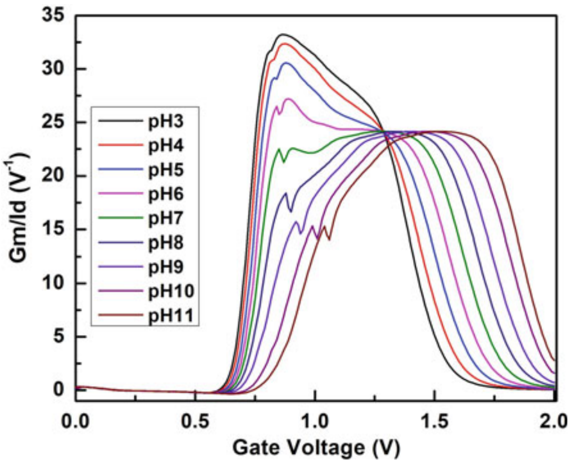

Fig. 10 Transconductance-to-current ratio curve at various pH values

ZnO-based ISFET can be employed in various fields, including life science, point-of-care testing (POCT) devices, medicine, and product safety. The ever-growing application of ZnO-based devices leads to the accumulation of zinc oxide (ZnO) nanomaterials that cause severe consequences to environment and human health. High-care of insulation and disposal must be taken care of while incorporating such devices in health care and environmental monitoring applications.

5 Conclusion

In this paper, the impact of ZnO as a sensing layer of a junctionless ISFET is studied over the various parameters (potential, drain current characteristics, transconductance, and sensitivity), and the results proved that ZnO is an effective sensitive material for detecting H^+ ions in an ISFET. The drain current characteristics show the pH-dependent behavior of a ZnO-based ISFET and confirm that this device can be used as a pH sensor. Polycrystalline ZnO-based TFT pH sensors show Nernst limit sensitivity besides the advantages of ease of fabrication and CMOS process compatibility. The simulated device shows excellent potential as a pH sensor.

References

1. M. Kaisti, Detection principles of biological and chemical fet sensors. Biosens. Bioelectron. **98**, 437–448 (2017)
2. N. Shafi, C. Sahu, C. Periasamy, Fabrication and ph sensitivity analysis of in-situ doped polycrystalline silicon thin-film junctionless biofet. IEEE Electron Device Lett. **40**, 997–1000 (2019)
3. A. Porwal, N. Shafi, C. Sahu, Fabrication and ph sensing characteristics measurement of back gate zno thin film planar fet. Silicon (2022)
4. M. Israr-Qadir, S. Jamil-Rana, O. Nur, M. Willander, Zinc oxide-based self- powered potentiometric chemical sensors for biomolecules and metal ions. Sensors **17**(7), (2017)
5. Y. Zhang, M.K. Ram, E.K. Stefanakos, D.Y. Goswami, Synthesis, charac- terization, and applications of zno nanowires. J. Nanomater. **2012**, 624520 (2012)
6. I. Ishteyaq, K. Muzaffar, Performance characterization of (pt, au, pd)/zno/n- si/al schottky structures for varied temperature and uv illumination conditions. Superlattices Microstruct. **145**, 106604 (2020)
7. K.S. Bhat, R. Ahmad, T. Mahmoudi, Y.-B. Hahn, High performance chemi- cal sensor with field-effect transistors array for selective detection of multiple ions. Chem. Eng. J. **417**, 128064 (2021)
8. J. Li, T. Rao, W. Liao, J. Jiang, P. Yang, J.J. Liou, Extended-gate field effect transistors with zinc oxide as sensing film for pH sensing, in *2021 9th International Symposium on Next Generation Electronics (ISNE)*, pp. 1–3 (2021)
9. T. Rao, J. Li, W. Cai, M. Wu, J. Jiang, P. Yang, Y. Zhou, W. Liao, Fabrication of a mesoporous multimetallic oxide-based ion-sensitive field effect transistor for pH sensing. ACS Omega **6**, 32297–32303 (2021)
10. N. Shafi, C. Sahu, C. Periasamy, Analytical modeling of surface potential and drain current for virtually doped symmetrical dielectric modulated biofet. IEEE Sens. J. **20**(9), 4749–4757 (2020)
11. D. Look, Recent advances in zno materials and devices. Mater. Sci. Eng. B **80**(1), 383–387 (2001)
12. N.R. Shanmugam, S. Muthukumar, S. Prasad, A review on zno-based elec- trical biosensors for cardiac biomarker detection. Future Sci. OA **3**(4), FSO196 (2017)
13. X. Ma, R. Peng, W. Mao, Y. Lin, H. Yu, Recent advances in ion-sensitive field-effect transistors for biosensing applications. Electrochem. Sci. Adv. e2100163
14. P. Bergveld, Development of an ion-sensitive solid-state device for neurophysiological measurements. IEEE Trans. Biomed. Eng. BME **17**(1), 70–71 (1970)
15. J.S. Parmar, C. Sahu, Cmos-compatible ex-situ incorporated junctionless enhancement-mode thin polysilicon film fet ph sensor. IEEE Trans. Device Mater. Reliab. **21**(1), 2–8 (2021)

16. E. Buitrago, M.F.-B. Badia, Y.M. Georgiev, R. Yu, O. Lotty, J.D. Holmes, A.M. Nightingale, H.M. Guerin, A.M. Ionescu, Electrical characterization of high performance, liquid gated vertically stacked sinw-based 3d fet biosensors. Sens. Actuators, B Chem. **199**, 291–300 (2014)
17. K.B. Oldham, A gouy–chapman–stern model of the double layer at a (metal)/(ionic liquid) interface. J. Electroanal. Chem. **613**(2), 131–138 (2008)
18. F. Pittino, P. Palestri, P. Scarbolo, D. Esseni, L. Selmi, Models for the use of commercial tcad in the analysis of silicon-based integrated biosensors. Solid-State Electron. **98**, 63–69 (2014)
19. R. Narang, M. Saxena, M. Gupta, Analytical model of ph sensing charac- teristics of junctionless silicon on insulator isfet. IEEE Trans. Electron Devices **64**(4), 1742–1750 (2017)
20. N. Shafi, A.M. Bhat, J.S. Parmar, C. Sahu, C. Periasamy, Effect of geometry and temperature variations on sensitivity and linearity of junctionless ph sensing fet: an experimental study. Micro Nanostruct **163**, 107186 (2022)
21. R. van Hal, J. Eijkel, P. Bergveld, A novel description of isfet sensitivity with the buffer capacity and double-layer capacitance as key parameters. Sens. Actuators, B Chem. **24**(1), 201–205 (1995)
22. D.E. Yates, S. Levine, T.W. Healy, Site-binding model of the electrical double layer at the oxide/water interface. J. Chem. Soc., Faraday Trans. 1 **70**, 1807–1818 (1974)
23. N. Miscourides, P. Georgiou, Isfet arrays in cmos: a head-to-head comparison between voltage and current mode. IEEE Sens. J. **19**(4), 1224–1238 (2019)
24. J. Go, P.R. Nair, M.A. Alam, Theory of signal and noise in double-gated nanoscale electronic pH sensors. J. Appl. Phys. **112**(3), 034516 (2012)
25. E. Mohammadi, N. Manavizadeh, An accurate tcad-based model for isfet simulation. IEEE Trans. Electron. Devices **65**(9), 3950–3956 (2018)
26. P. Dwivedi, A. Kranti, Applicability of transconductance-to-current ratio (g_m/i_{ds}) as a sensing metric for tunnel fet biosensors. IEEE Sens. J. **17**(4), 1030–1036 (2017)